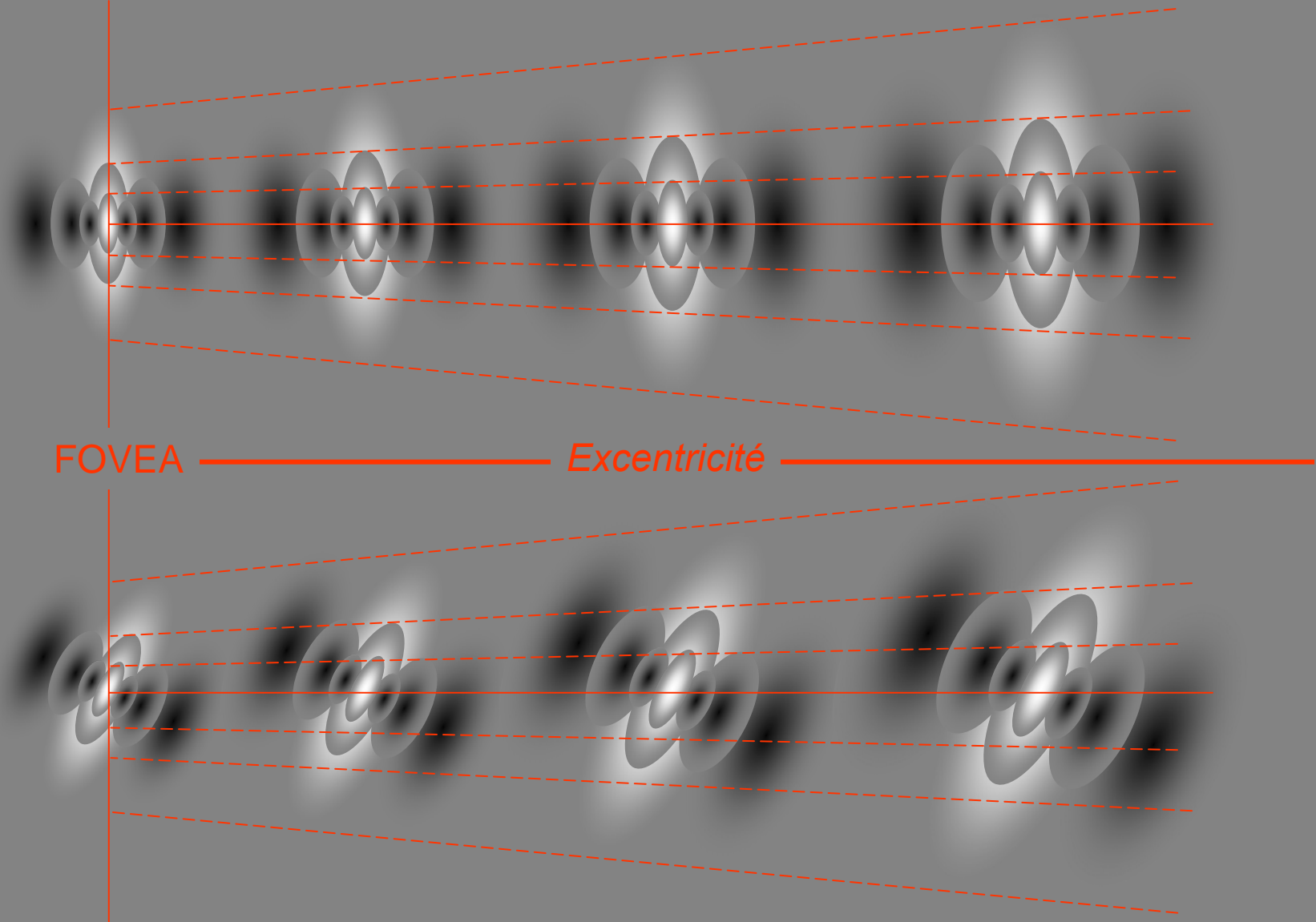
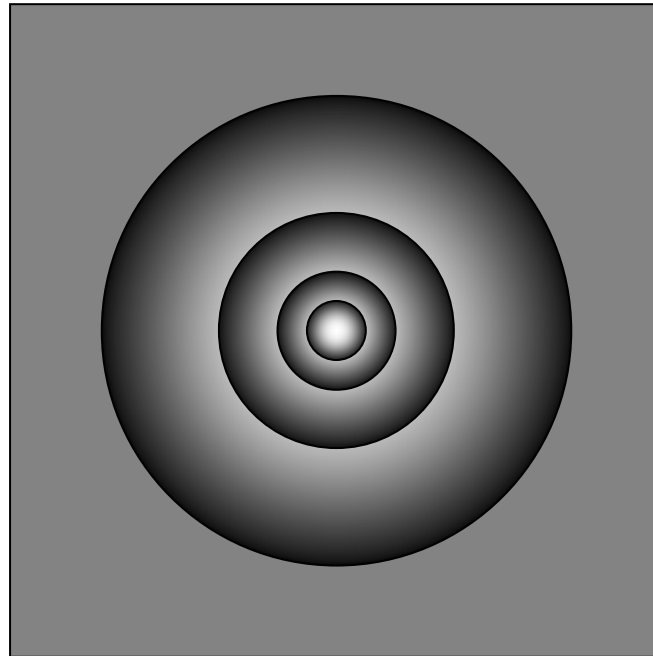


REPRESENTATION 'MULTIECHELLE' DE CHAQUE POINT RETINIEN



The Laplacian Pyramid as a Compact Image Code

PETER J. BURT, MEMBER, IEEE, AND EDWARD H. ADELSON



GAUSSIAN PYRAMID

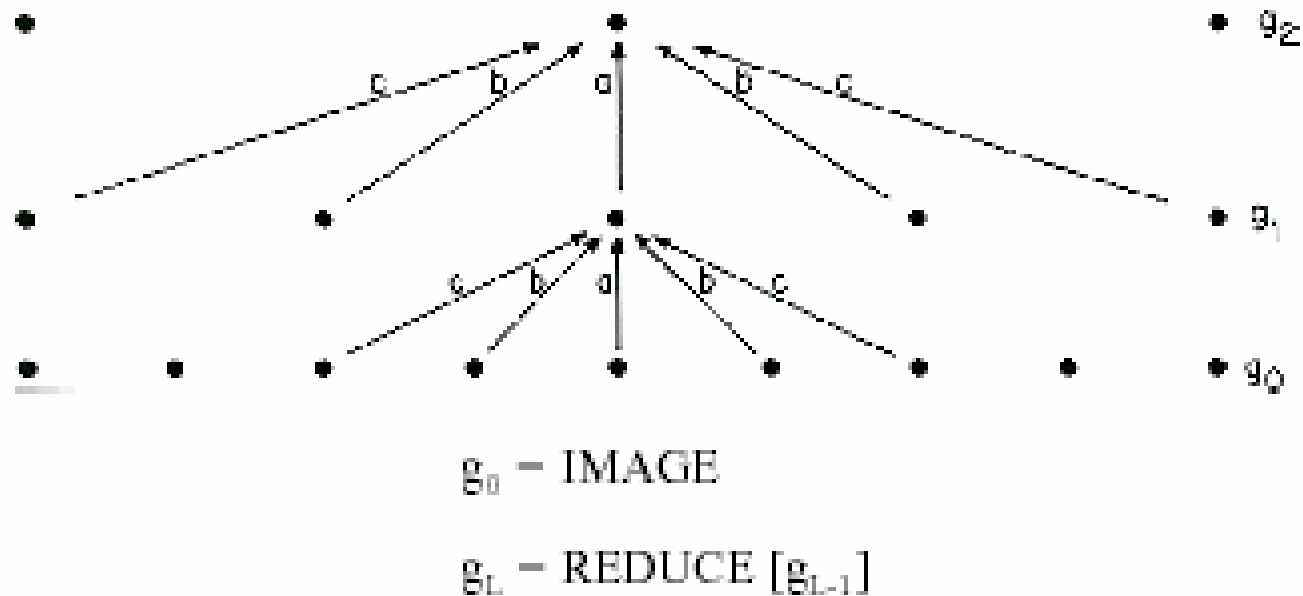


Fig 1. A one-dimensional graphic representation of the process which generates a Gaussian pyramid. Each row of dots represents nodes within a level of the pyramid. The value of each node in the zero level is just the gray level of a corresponding image pixel. The value of each node in a high level is the weighted average of node values in the next lower level. Note that node spacing doubles from level to level, while the same weighting pattern or "generating kernel" is used to generate all levels.

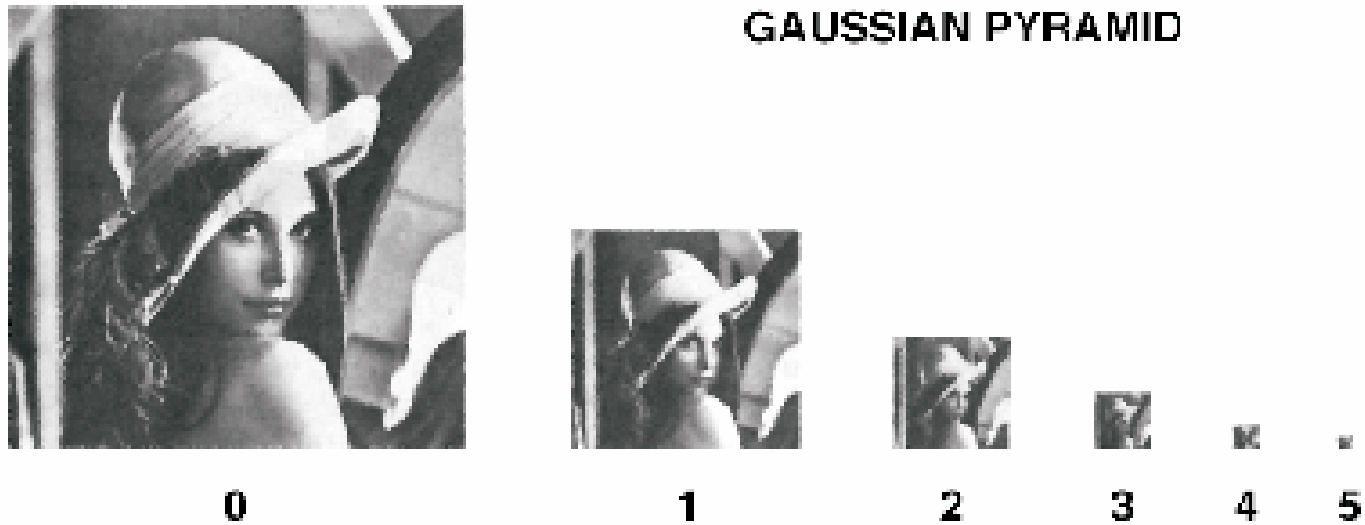


Fig. 4. First six levels of the Gaussian pyramid for the "Lady" image. The original image, level 0, measures 257 by 257 pixels and each higher level array is roughly half the dimensions of its predecessor. Thus, level 5 measures just 9 by 9 pixels.

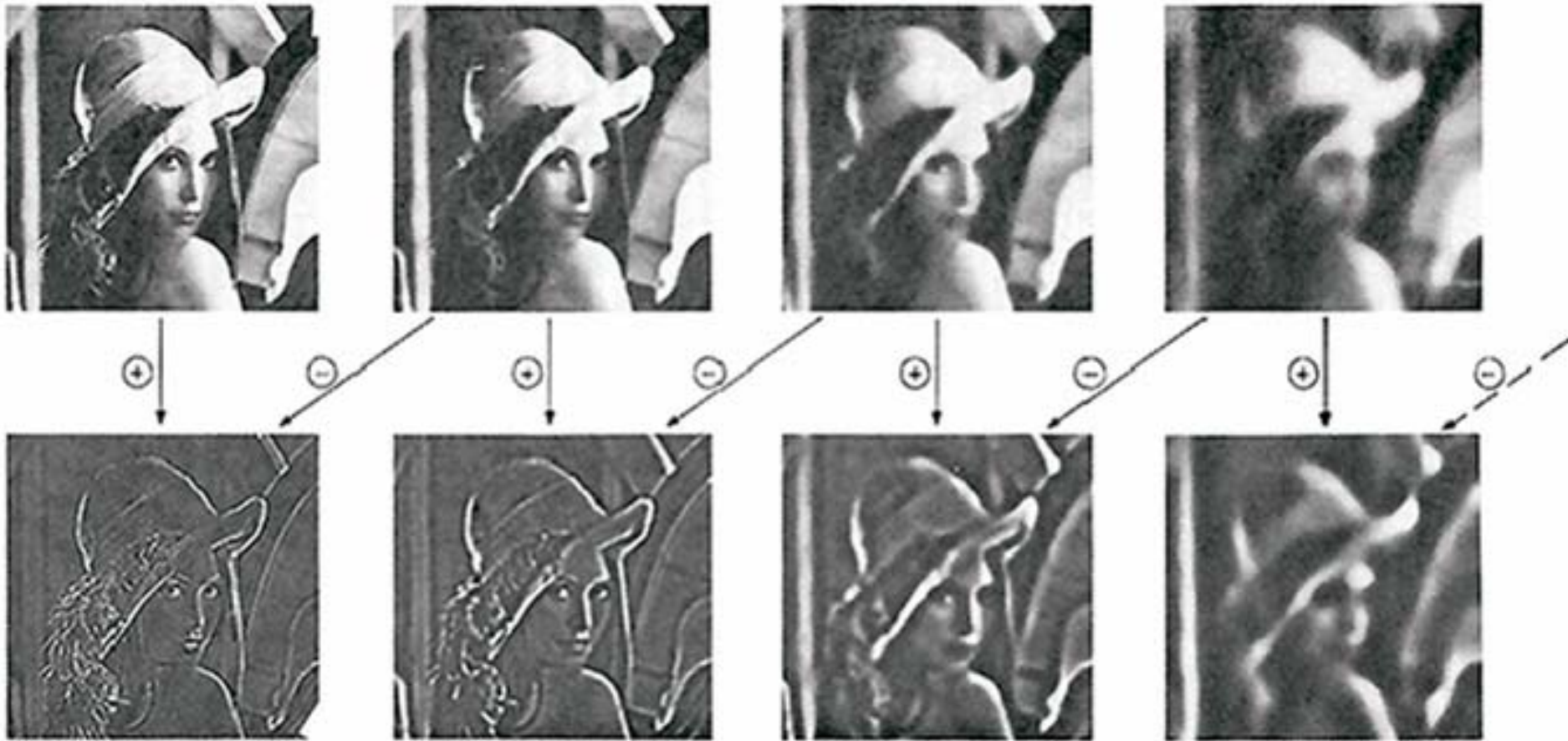
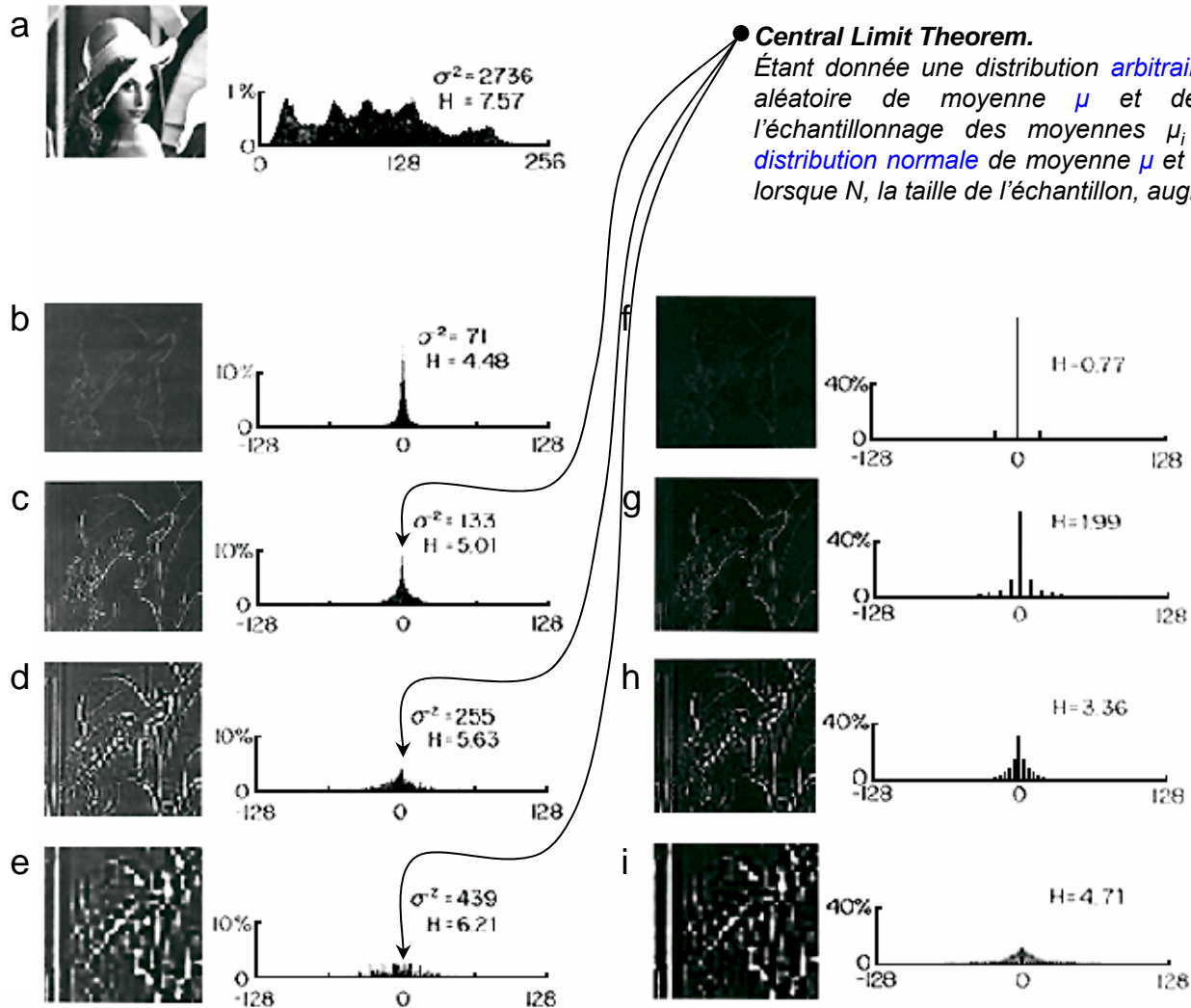


Fig 5. First four levels of the Gaussian and Laplacian pyramid. Gaussian images, upper row, were obtained by expanding pyramid arrays (Fig. 4) through Gaussian interpolation. Each level of the Laplacian pyramid is the difference between the corresponding and next higher levels of the Gaussian pyramid.



Central Limit Theorem.

Étant donnée une distribution *arbitraire* d'une variable aléatoire de moyenne μ et de variance σ^2 , l'échantillonnage des moyennes μ_i tend vers une *distribution normale* de moyenne μ et de variance σ^2/N lorsque N , la taille de l'échantillon, augmente.

FIG 6. The distribution of pixel gray level values at various stages of the encoding process. The histogram of the original image is given in (a). (b)-(e) give histograms for levels 0-3 of the Laplacian pyramid with generating parameter $a=0.6$. Histograms following quantization at each level are shown in (f)-(i). Note that pixel values in the Laplacian pyramid are concentrated near zero, permitting data 5 compression through shortened and variable length code words. Substantial further reduction is realized through quantization (particularly at low pyramid levels) and reduced sample density (particularly at high pyramid levels).

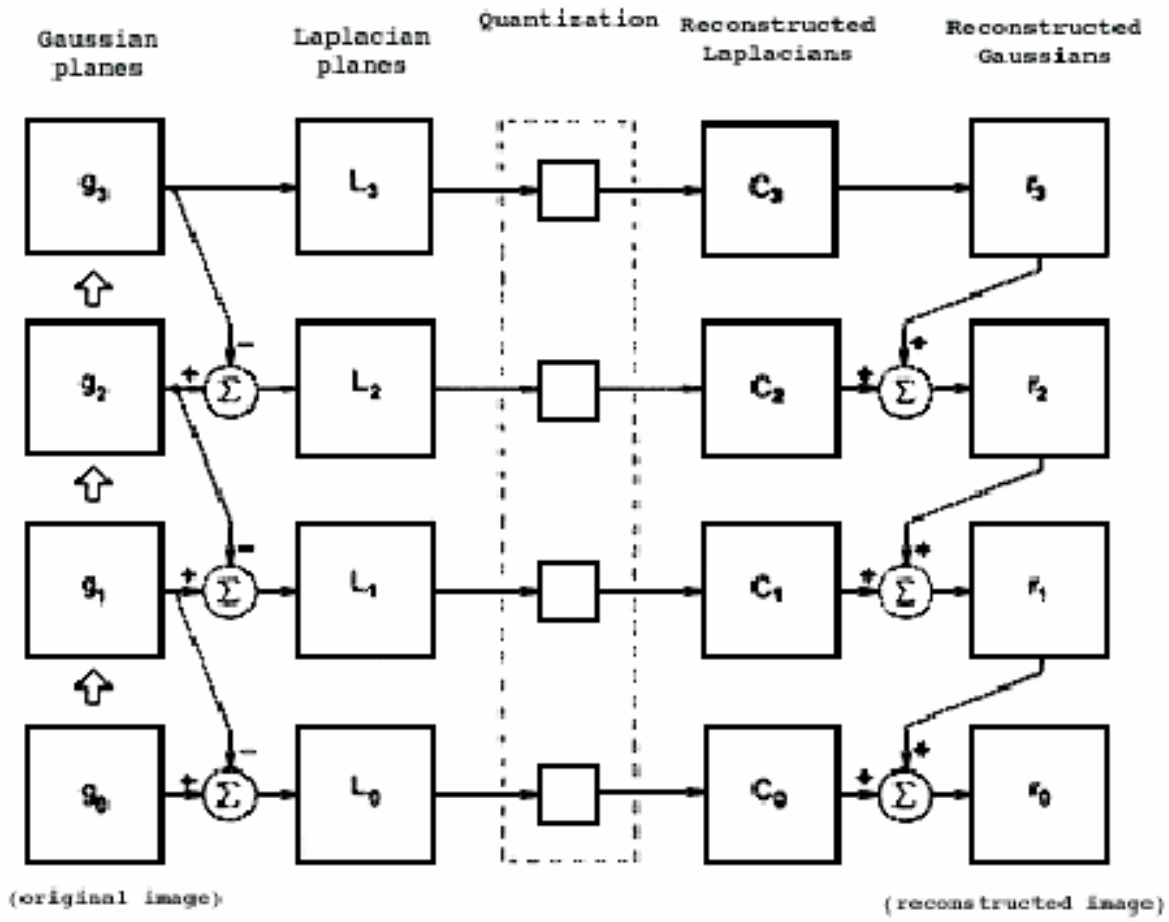


Fig. 10. A summary of the steps in Laplacian pyramid coding and decoding. First, the original image g_0 (lower left) is used to generate Gaussian pyramid levels g_1, g_2, \dots through repeated local averaging. Levels of the Laplacian pyramid L_0, L_1, \dots are then computed as the differences between adjacent Gaussian levels. Laplacian pyramid elements are quantized to yield the Laplacian pyramid code C_0, C_1, C_2, \dots . Finally, a reconstructed image r_0 is generated by summing levels of the code pyramid.

Sagi, D. (1995). The psychophysics of texture segregation. In T.V. Papathomas, C. Chubb, A. Gorea & E. Kowler (Eds.) *Early vision and beyond*. MIT Press, Cambridge.

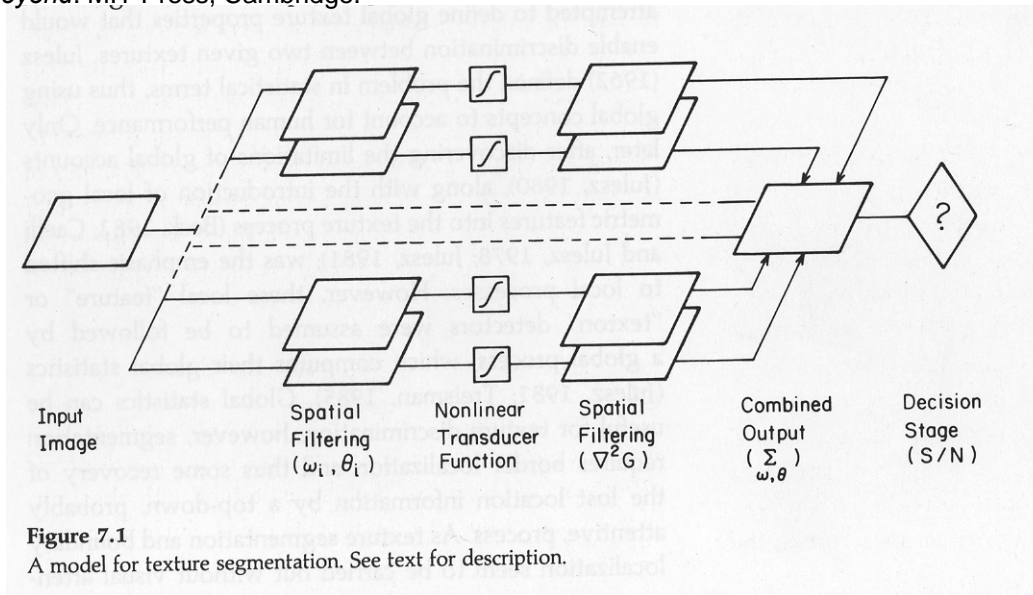
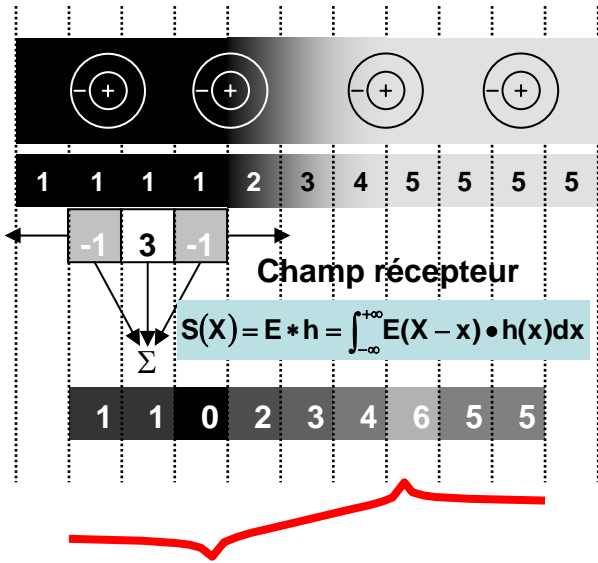


Fig. 17.3
Gaussian pyramid computation illustrated using a picture of Alan Turing. Each picture is produced by applying a small Gaussian-like filter to the previous output, followed by subsampling by a factor of two in each direction.

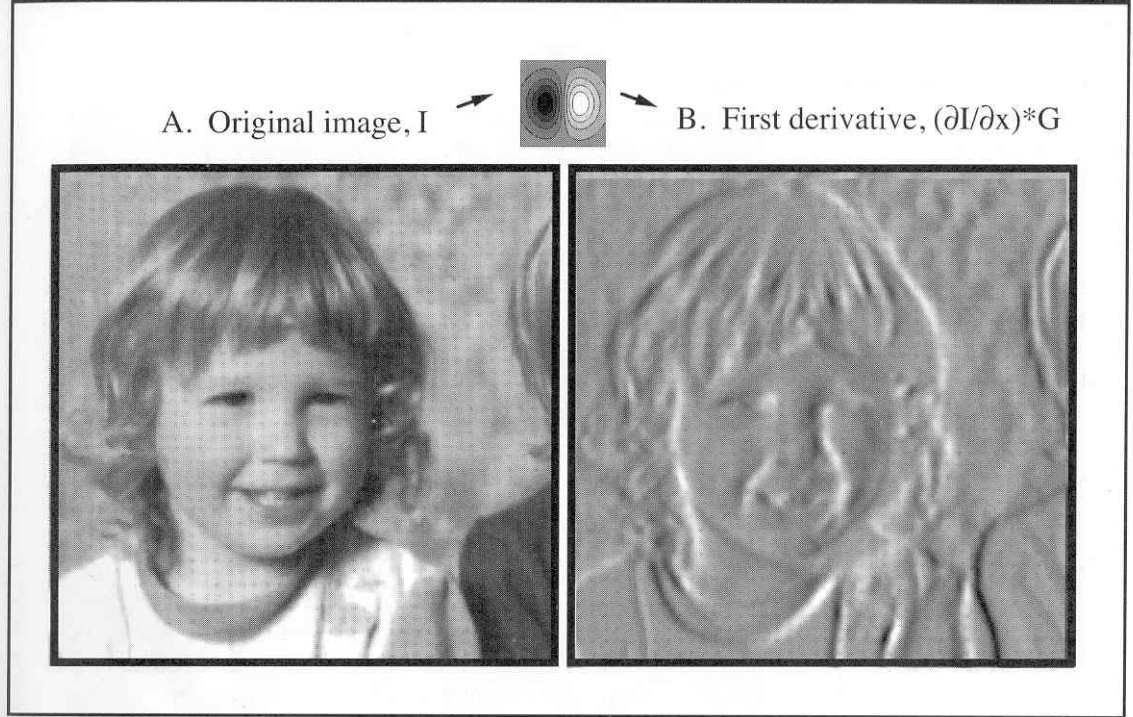
Bergen, J.R. & Landy, M.S. (1991). Computational modeling of visual texture segregation. In M.S. Landy & J.A. Movshon (Eds.) *Computational models of visual processing*. MIT Press, Cambridge.

CONVOLUTION



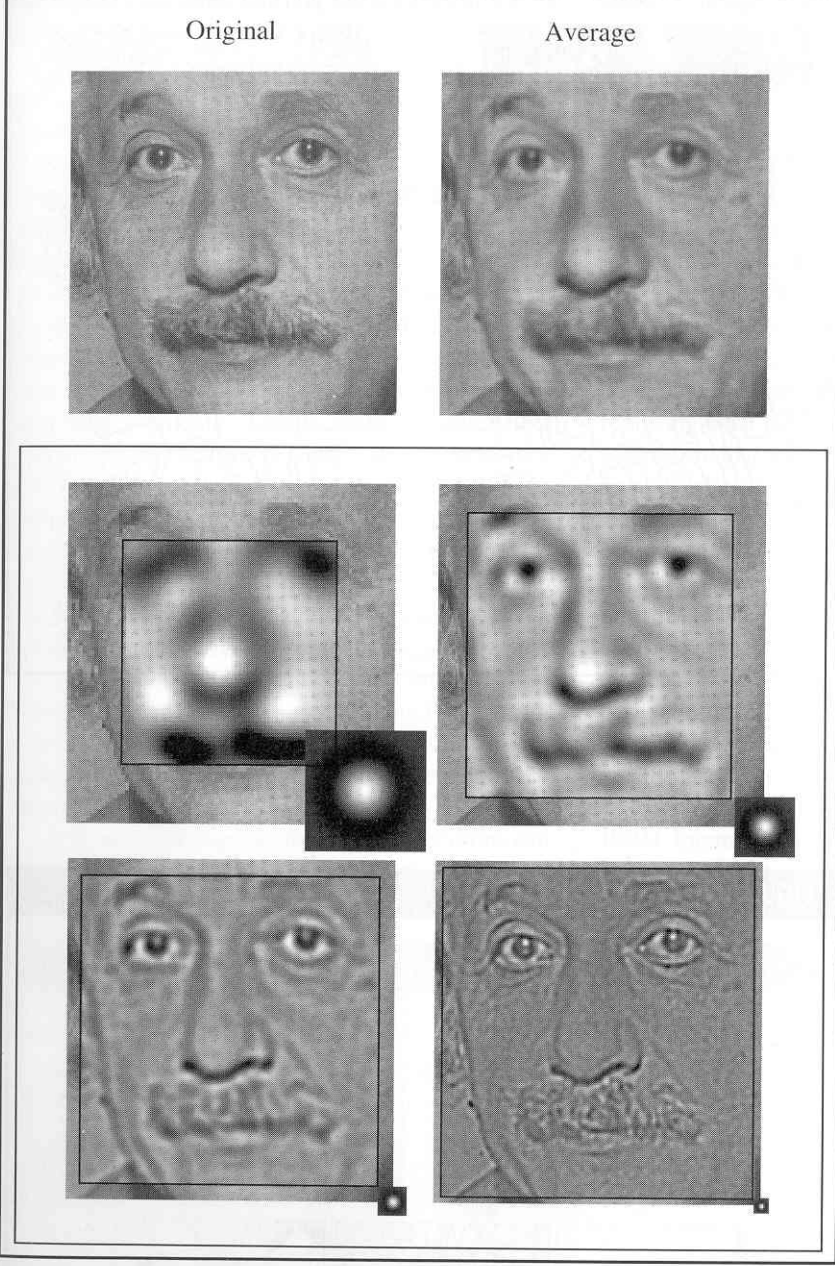
$$S(X) = E * h = \int_{-\infty}^{+\infty} E(X-x) \cdot h(x) dx$$

FIGURE 5.2



Edges and gradients in images. (A) Original image. (B) Filtered image that highlights the places that have a steep gradient in a horizontal direction. Light points have a steep positive gradient; dark points have a steep negative gradient. Notice how these points are associated with vertical or near-vertical edges in the original. The filter's receptive field (inset, enlarged $\times 4$) combined two operations—smoothing by a Gaussian filter (G) and differentiation (d/dx).

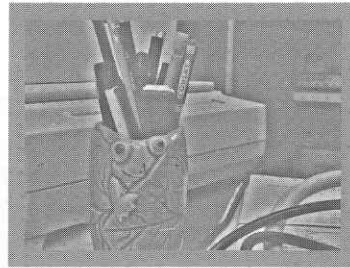
FIGURE 5.4



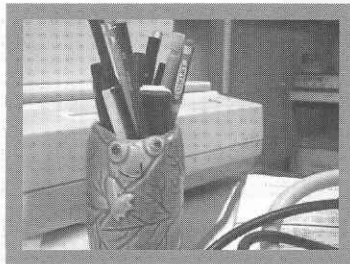
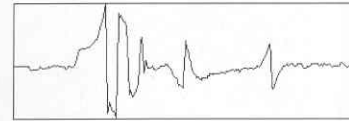
Example of spatial filtering at multiple spatial scales. Top left: Original image. Below: four filtered images obtained using circular, Laplacian-of-Gaussian, centre-surround receptive fields. The receptive fields, shown attached to each image, ranged from large to small. Note that the filter output is shown only within the black outlines. Top right: average of the four filtered images. The similarity between this and the original image shows that multiscale filtering can preserve all the image information, even though any one scale does not.

FIGURE 2.13

Spatial filtering of an image.
(A) A high-pass filtered version of the original (B), with low frequencies suppressed, as in Fig. 2.12C.
(C) The complementary, low-pass filtered image, with high frequencies suppressed. In fact, (C) was produced by blurring the image directly, to average or smooth out the higher frequencies, and (A) was formed by subtracting the low frequencies (C) from the original (B), i.e. $B = A + C$. Graphs show the intensity profile of a horizontal slice through the centre of each image. Note the smoothness of (C) and the lack of large-scale differences in (A).



A. High-pass filtered



B. Original

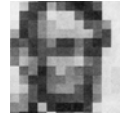
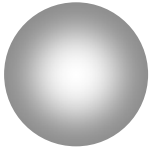


C. Low-pass filtered

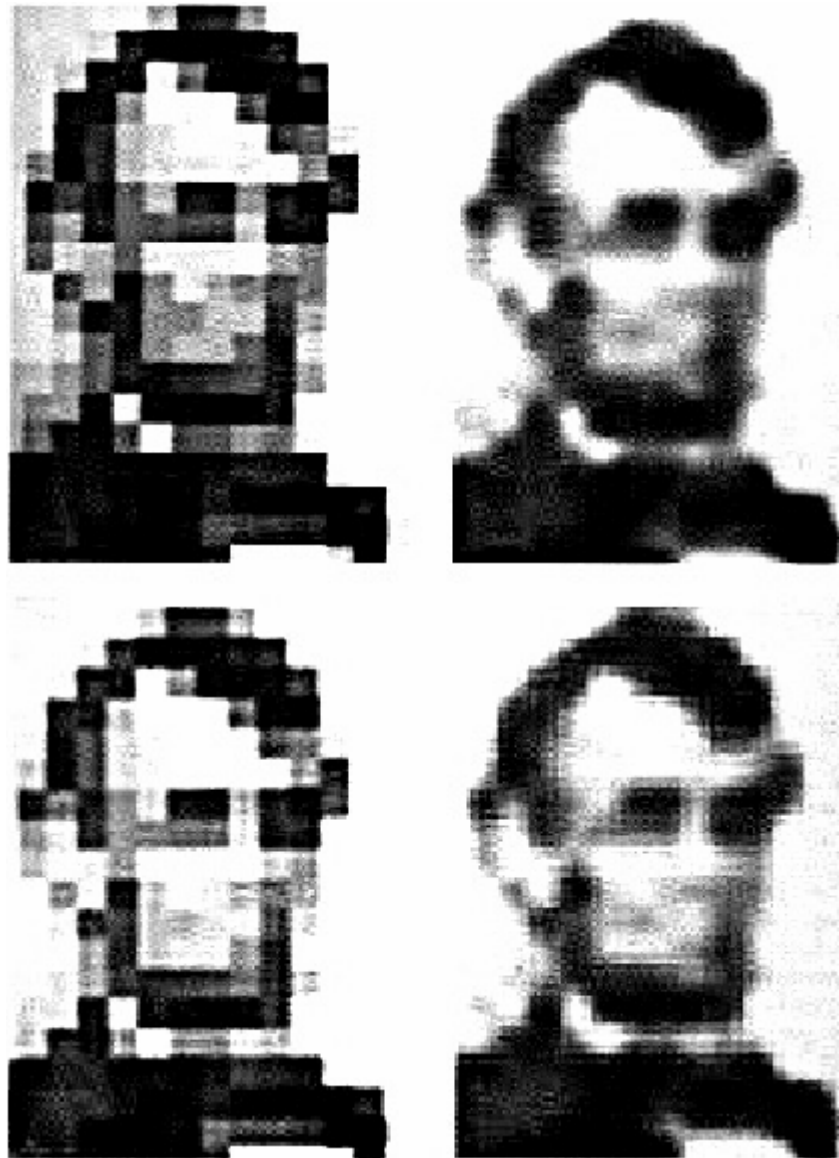




Seurat (1859-1891);
Grand champ, 1885.



Harmon, L. & Julesz, B. (1973). Masking in Visual recognition: Effects of Two-Dimensional Noise. *Science* 180, 1194

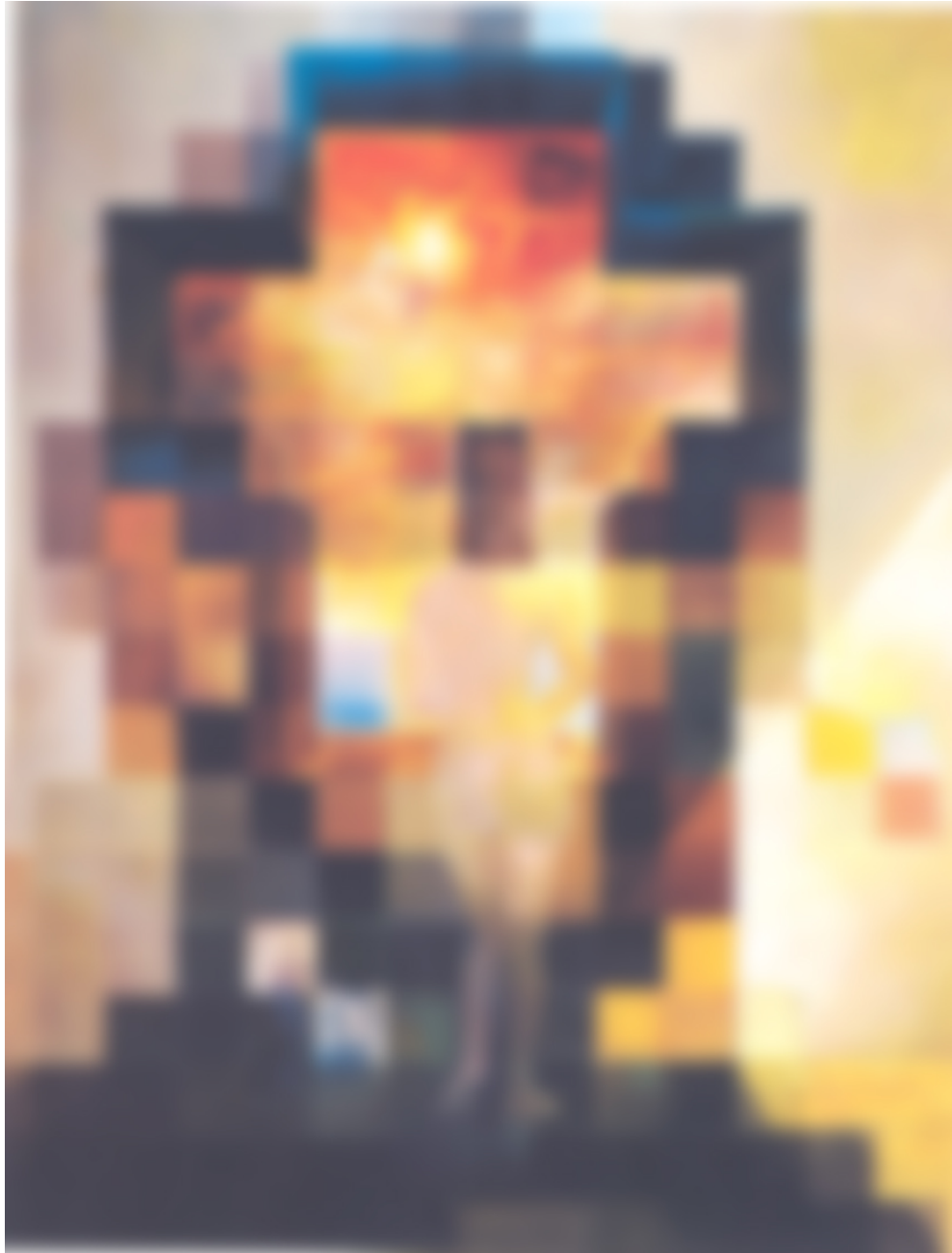
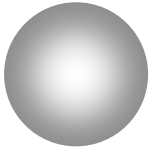


The top left image is the untouched block portrait

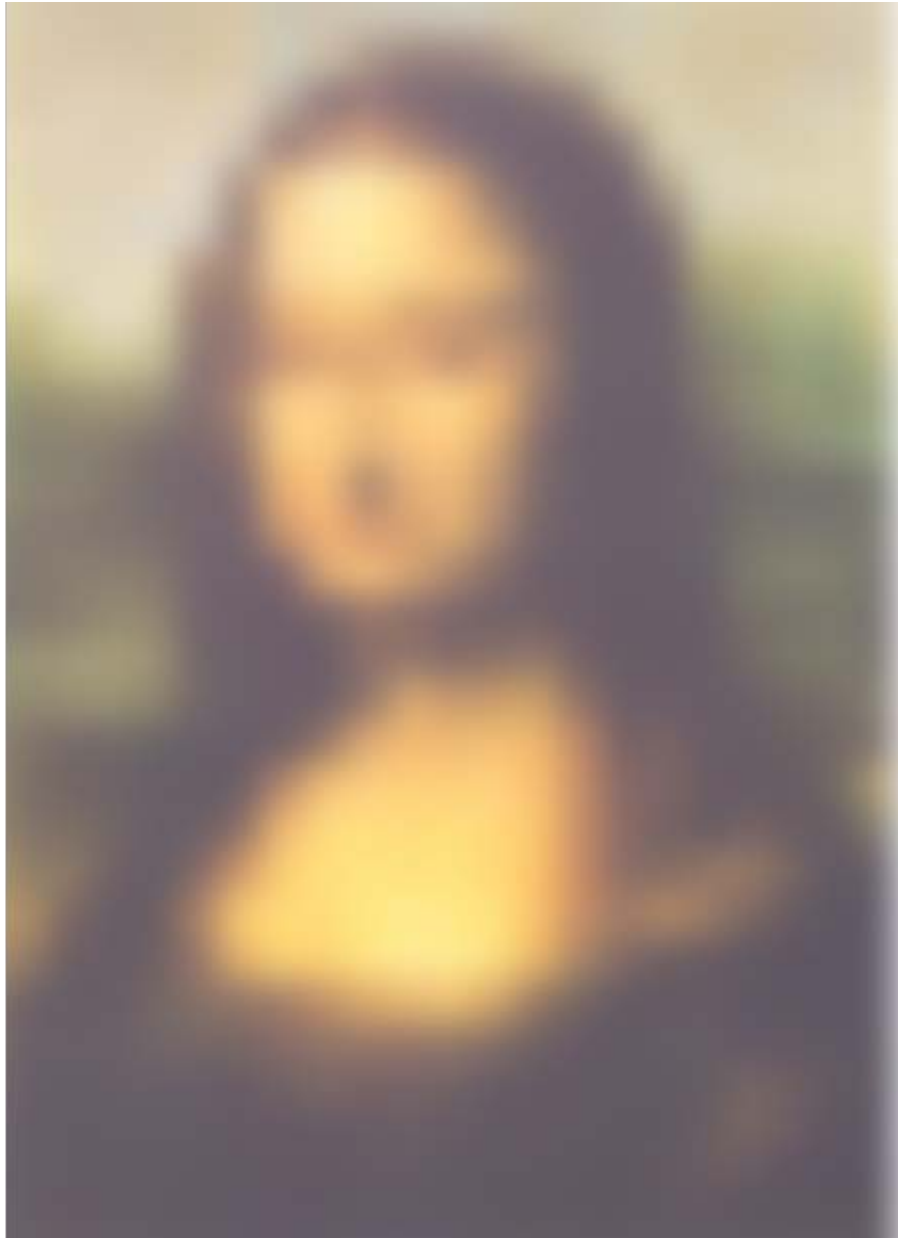
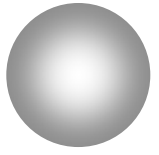
Top right is the portrait that is more identifiable through blurring

Bottom right has the high frequencies removed with no enhancement of identifiability

Bottom left has the frequencies near the critical band removed with an enhancement in identifiability

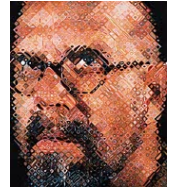
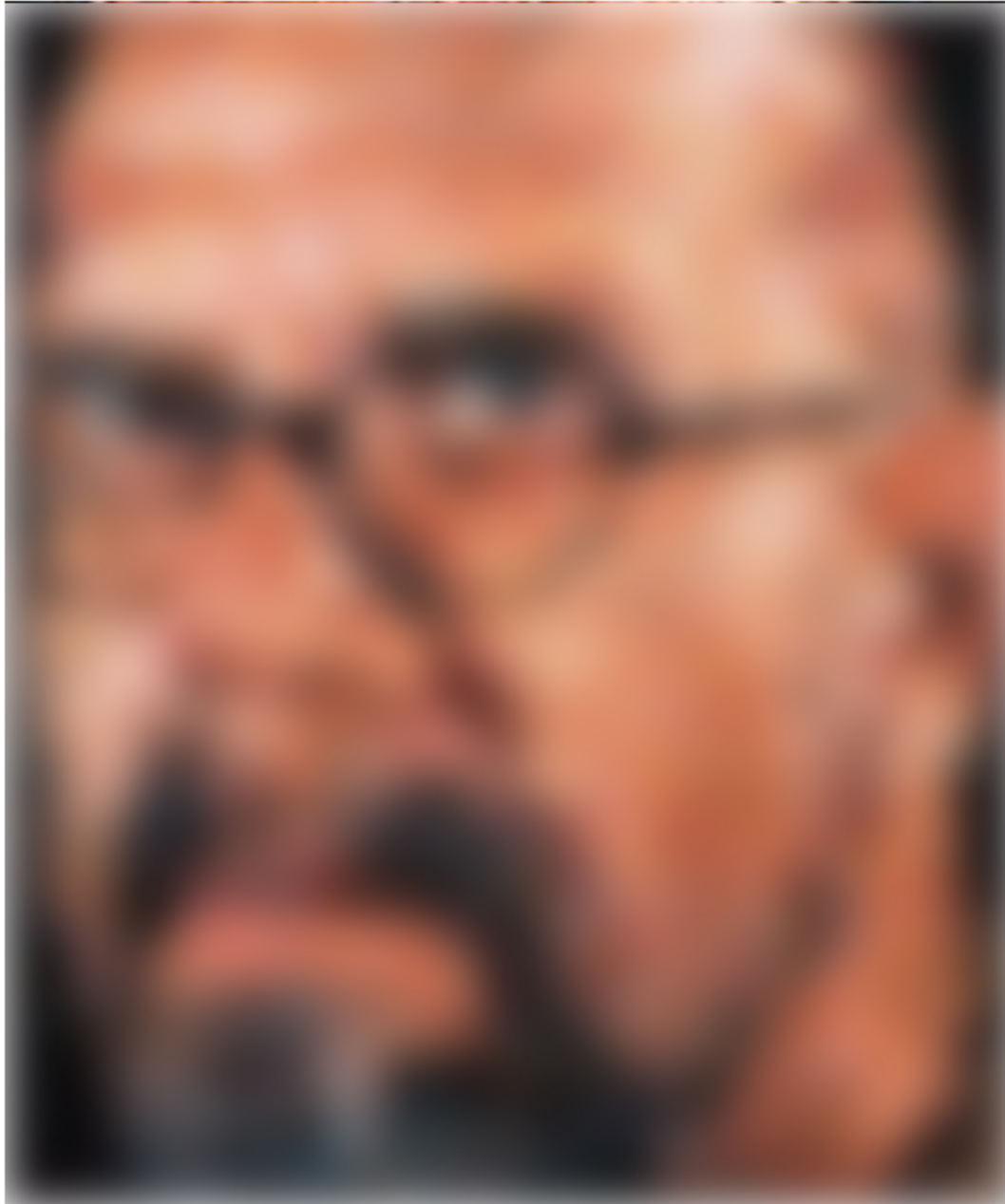
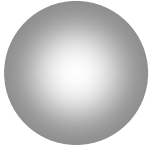


Dali

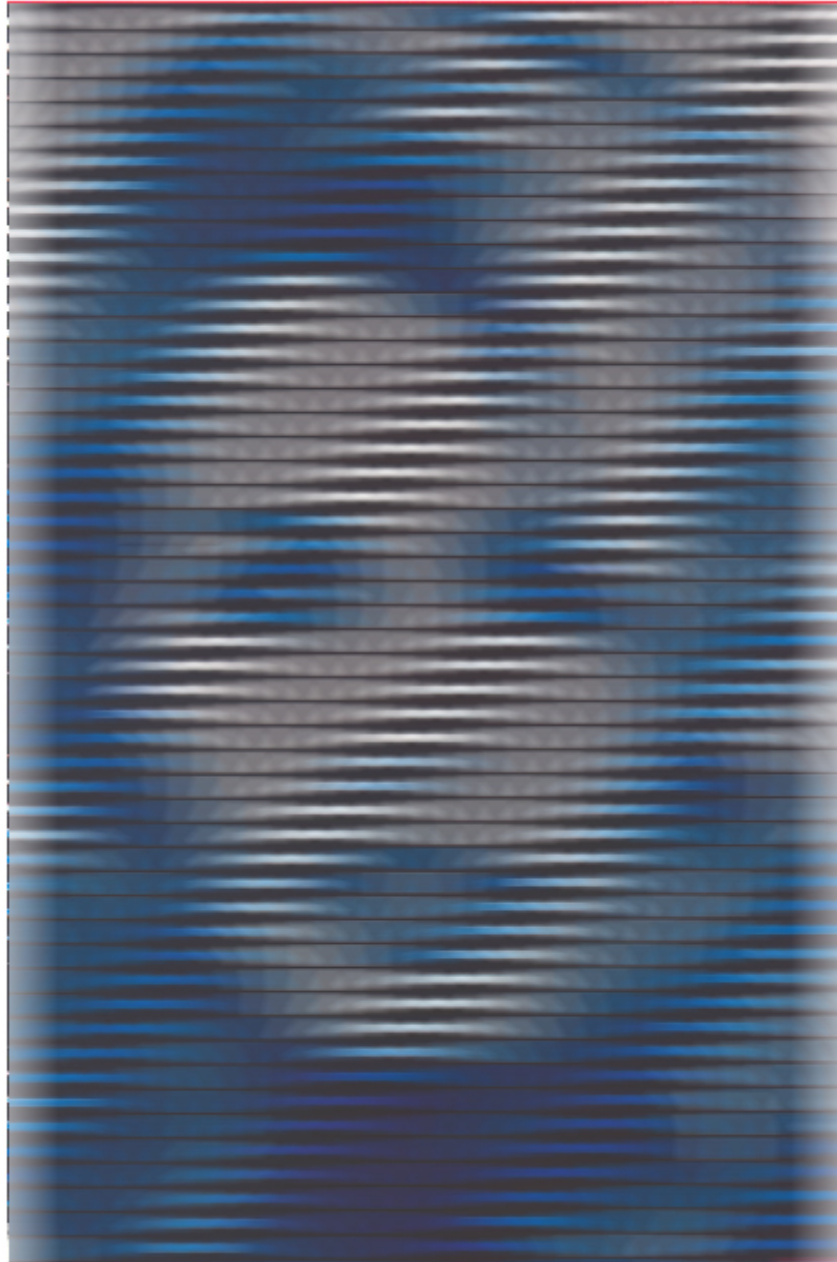
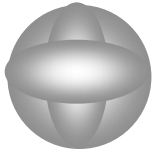


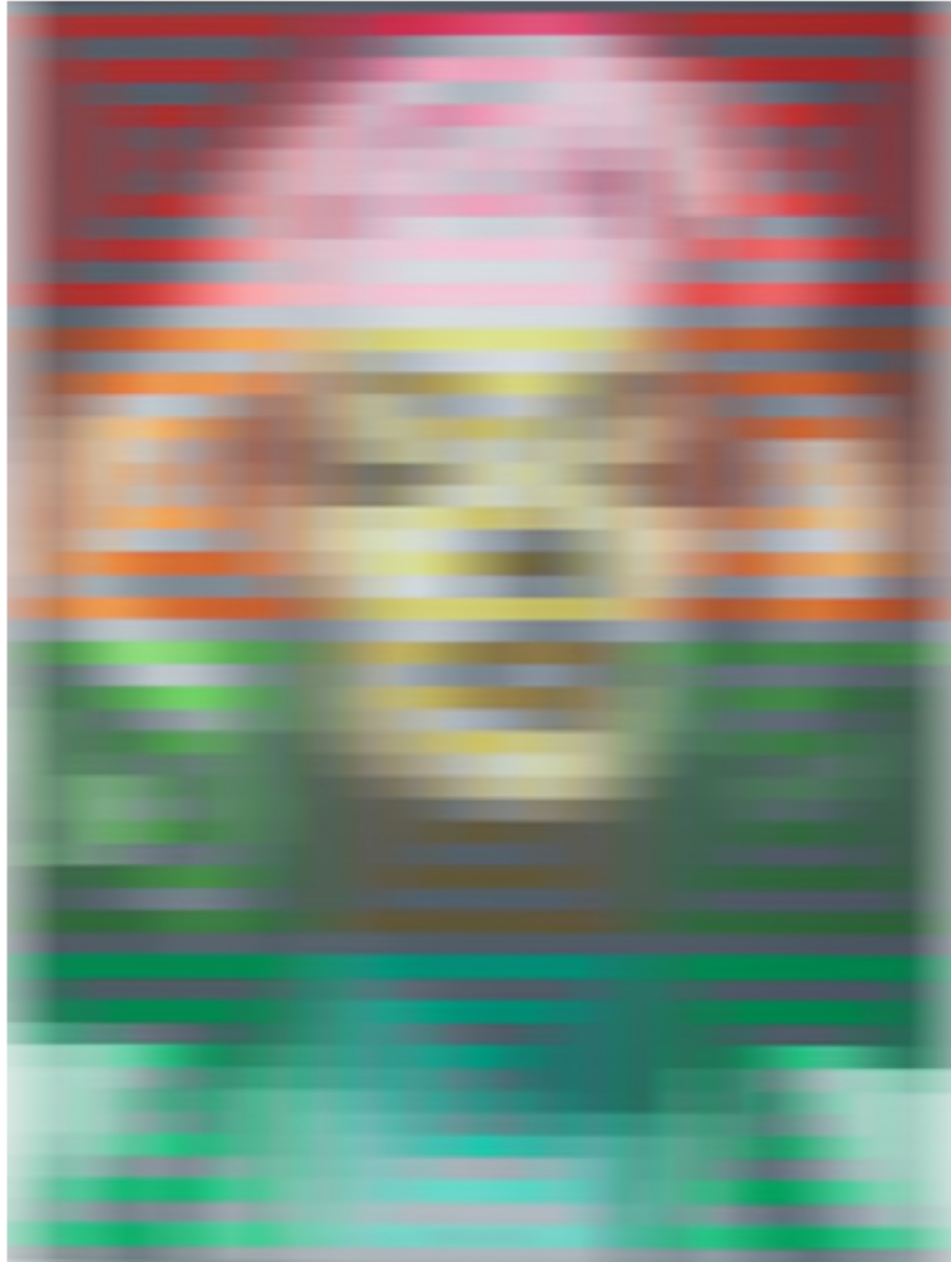
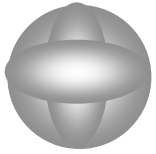


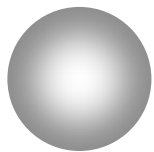
Chuck Close



Chuck Close





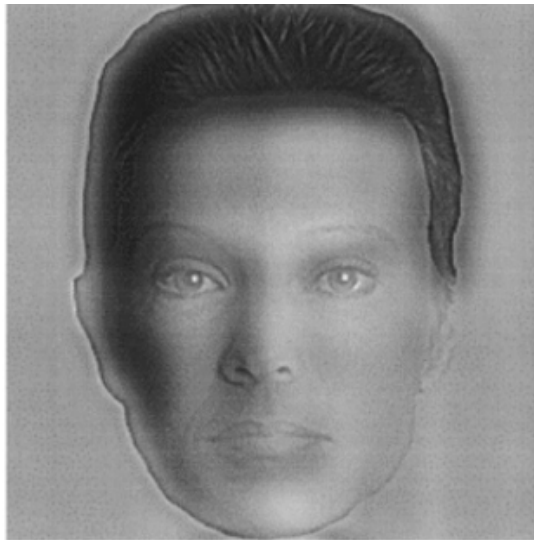


Yvaral : *Dali*

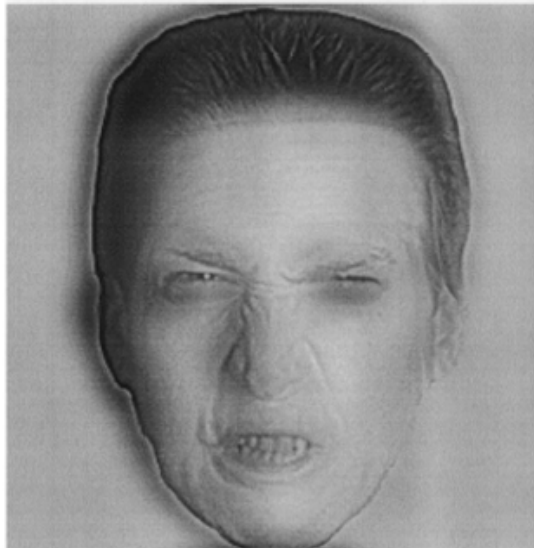
Low Spatial Frequency: Margaret Thatcher
High Spatial Frequency: Tony Blair



An hybrid face presenting Margaret Tatcher (in Low Spatial Frequency) and Tony Blair (High Spatial Frequency) has been displayed in 1998 in the Scottish National Portrait Gallery in Edinburgh (" The Science of the Face" organized by V. Bruce and A. Young). If you squint, blink or defocus while looking at the pictures, Margaret Tatcher should substitute for Tony Blair (if this demonstration does not work, step back from the pictures until your percepts change). The right picture is published in the book "In The Eye of the Beholder: the Science of Face Perception", Vicki Bruce and Andy Young (Eds.), Oxford, 1998 (p 64).



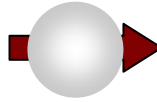
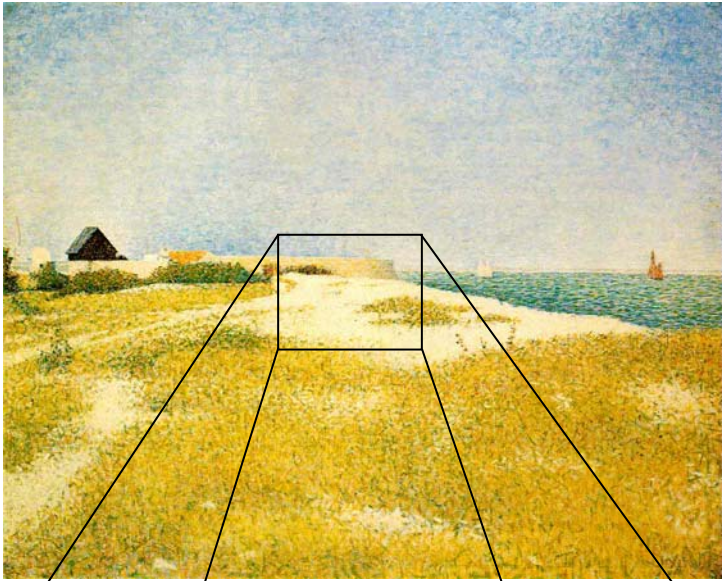
HSF: neutral woman;
LSF: angry man.



HSF: angry man;
LSF: neutral woman.

Fig. 1. Two of the hybrid faces used in expts 1, 2 & 3. The fine spatial scales (HSF) represents a non-expressive woman in the top picture and an angry man in the bottom picture. The coarse spatial scale (LSF) represents the angry man in the top picture and the neutral woman in the bottom picture. To see the LSF faces, squint, blink, or step back from the picture until your perception changes.

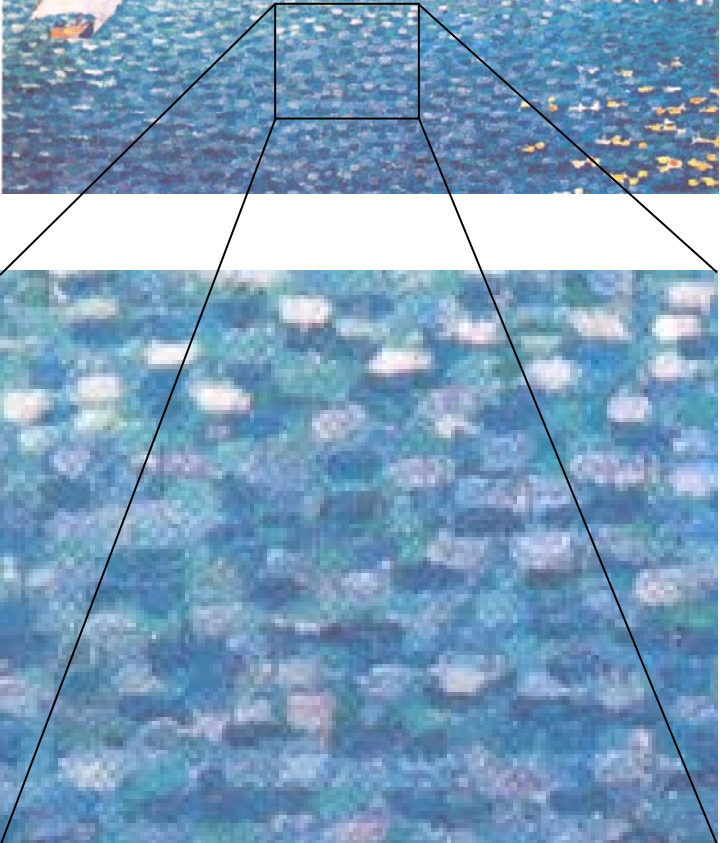
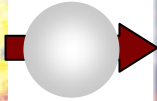
Schyns P.G. & Oliva A. (1999) Dr. Angry and Mr. Smile: when categorization flexibly modifies the perception of faces in rapid visual presentations. *Cognition*, 69, 243-2625.



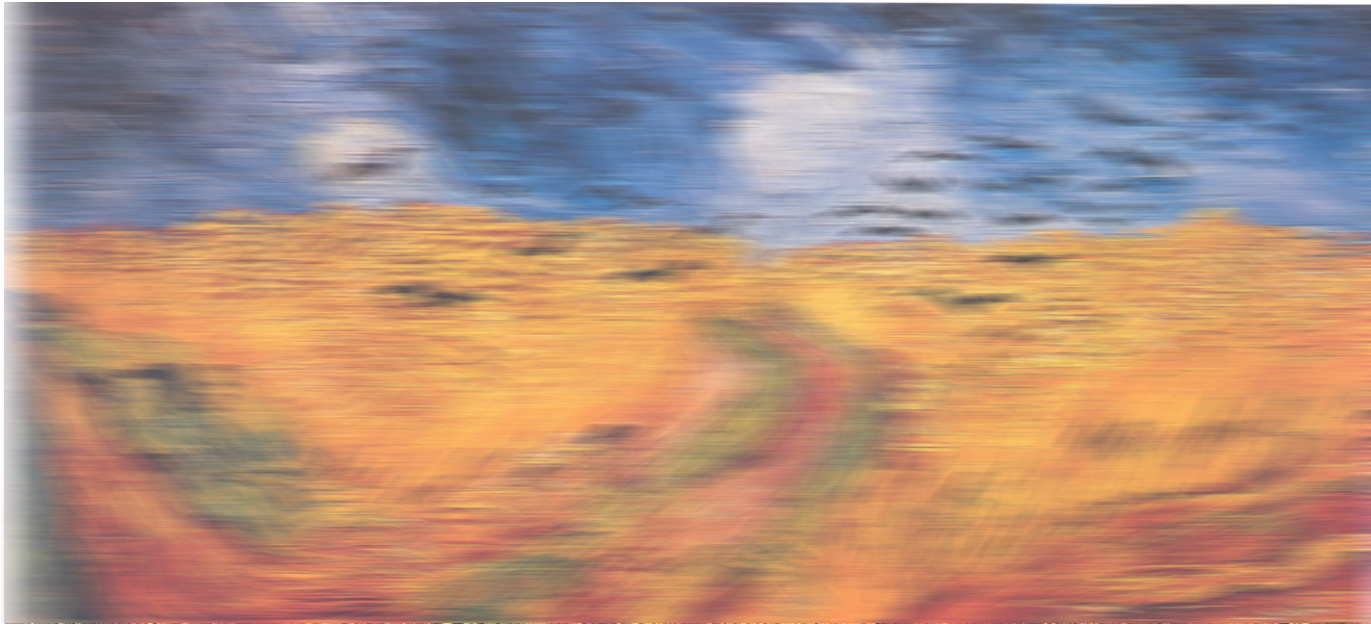
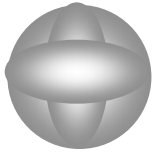
Seurat



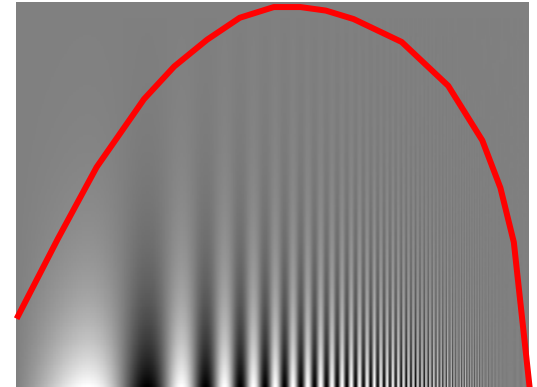
Signac



Signac



Van Gogh



From left to right each column contains noise of higher and higher frequency. From top to bottom are letters that are decreasing in their contrast. Effectiveness of the mask is determined by how far down one can identify in a column. The reason you cannot read very far down the center column is because the critical band for identifying letters is sensitive to the frequency of the noise.

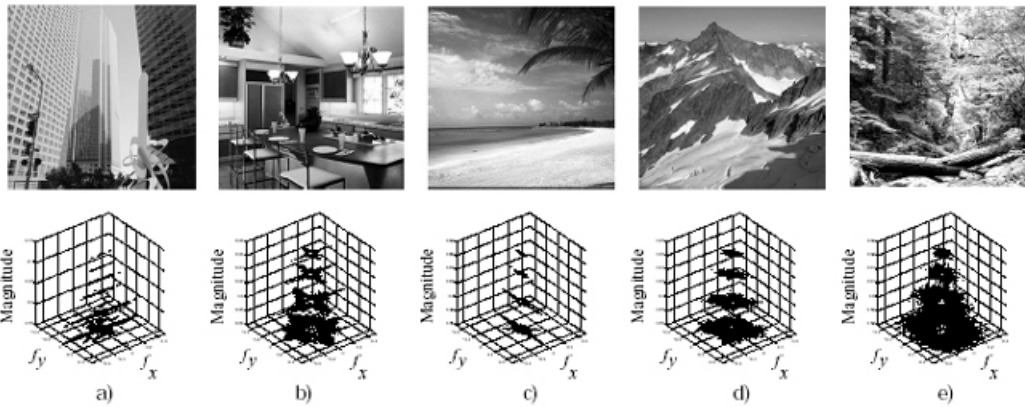


Fig. 1. Examples of power spectrum forms for prototypical images (vertical axis is the magnitude in log scale, horizontal axes are the spatial frequencies f_x & f_y). At the bottom, we show sections at several levels of the power spectrum of each image.

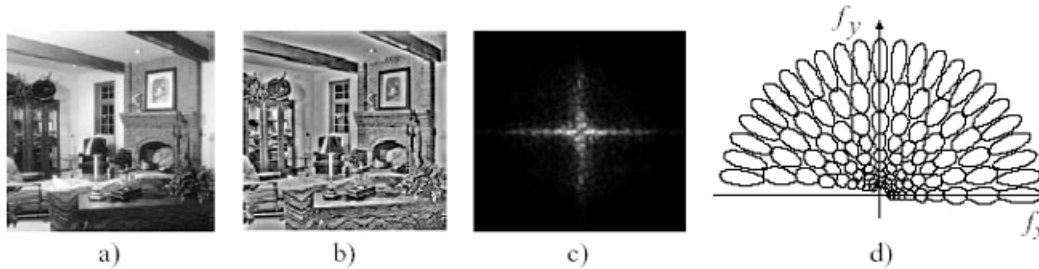


Fig. 2. The main steps for computing the vector of 100 components used to represent an image. a) Original image. b) Output of the preprocessing stage: the effect of illuminant and shadows have been reduced. c) Power spectrum of the prefiltered image. It is computed as the square of the magnitude of the Fourier Transform. d) -3dB sections of the set of Gabor filters used to sample the power spectrum. The highest frequency is 1/3 cycles/image and the lowest one is 1/72 cycles/image.

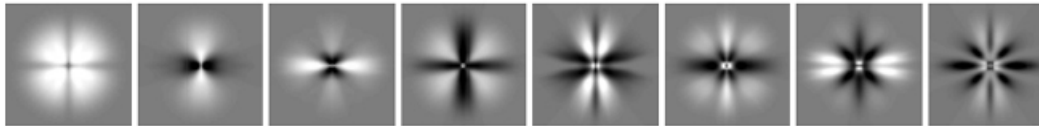


Fig. 3. The first 8 Principal components calculated from the spectrum of 700 scenes. The horizontal coordinate is f_x and the vertical one is f_y . The symmetrical structure of the principal components is due to the mirror transformation applied to the image power spectrum.

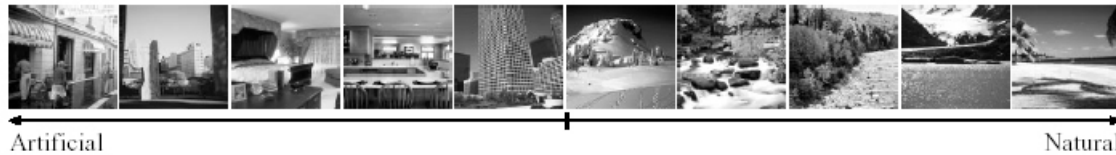


Fig. 5. Organization of new prototypical scenes on the Artificial-Natural axis. Pictures have been randomly selected and are equally spaced along the axis. The left side exhibits artificial scenes and the right side exhibits natural scenes.



Fig. 6. Examples of ambiguous scenes and their organization along the Artificial-Natural axis. Images are sorted according to the Artificial-Natural DST (*Discriminant Spectral Template*). From the top to bottom & from the left to the right, scenes are organized from the most artificial to the most natural. Underlined images belong to the prototypical groups.

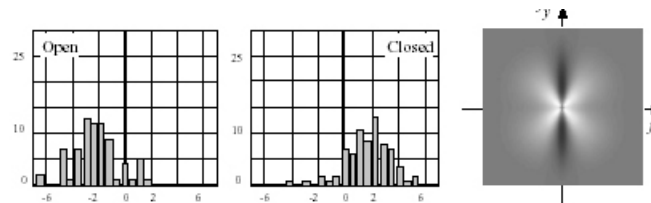


Fig. 7. Results of projection of the testing group of natural images onto the Open-Closed axis. On the right-hand side we show the resulting DST. 88% of the images are well classified in the learning and the testing phases.



Fig. 8. Organization of new scenes randomly selected from the testing group along the Open-Closed axis.

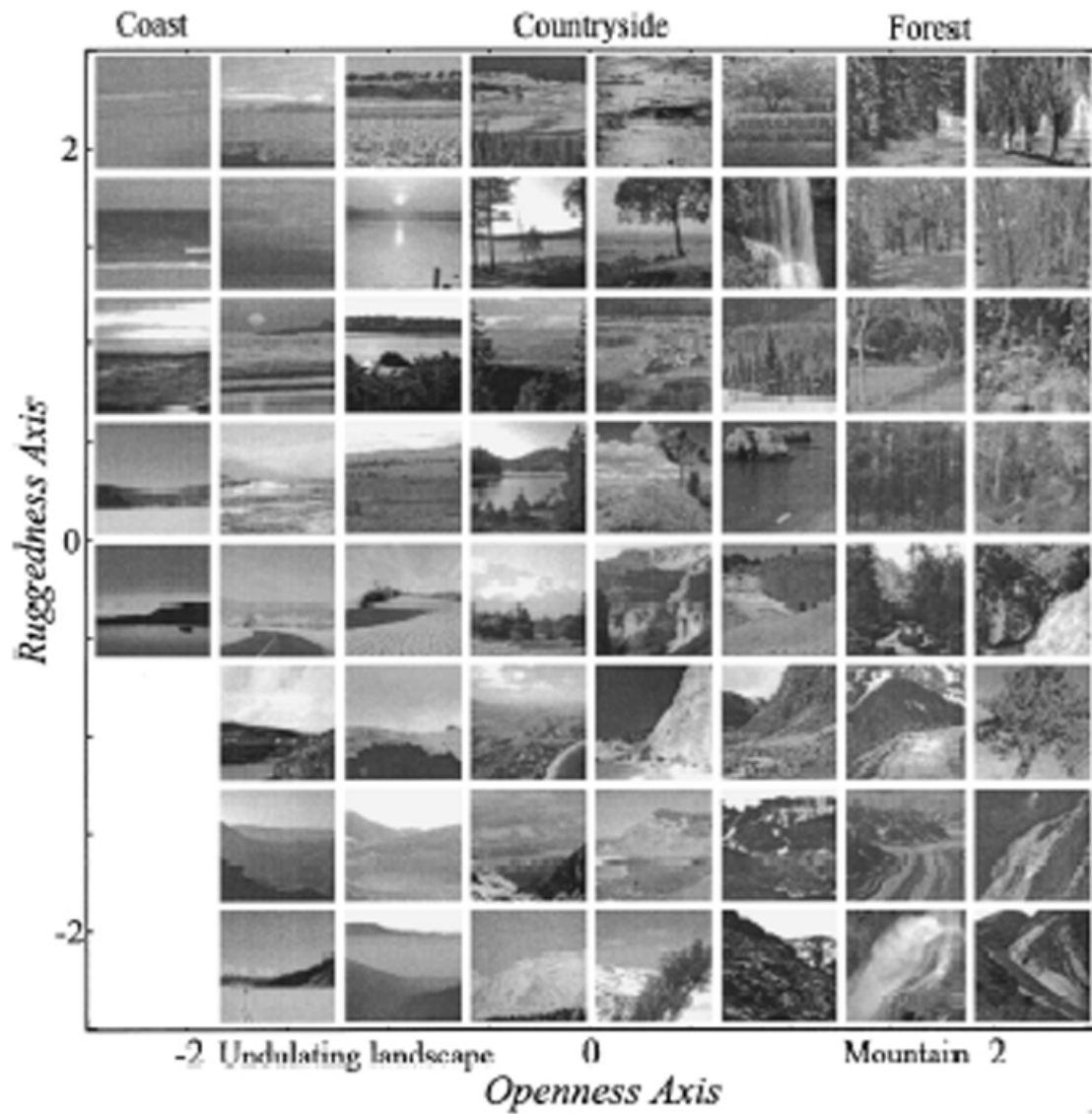


Fig. 15. Organization of new scenes according to the openness and ruggedness properties extracted by the WDSTs.

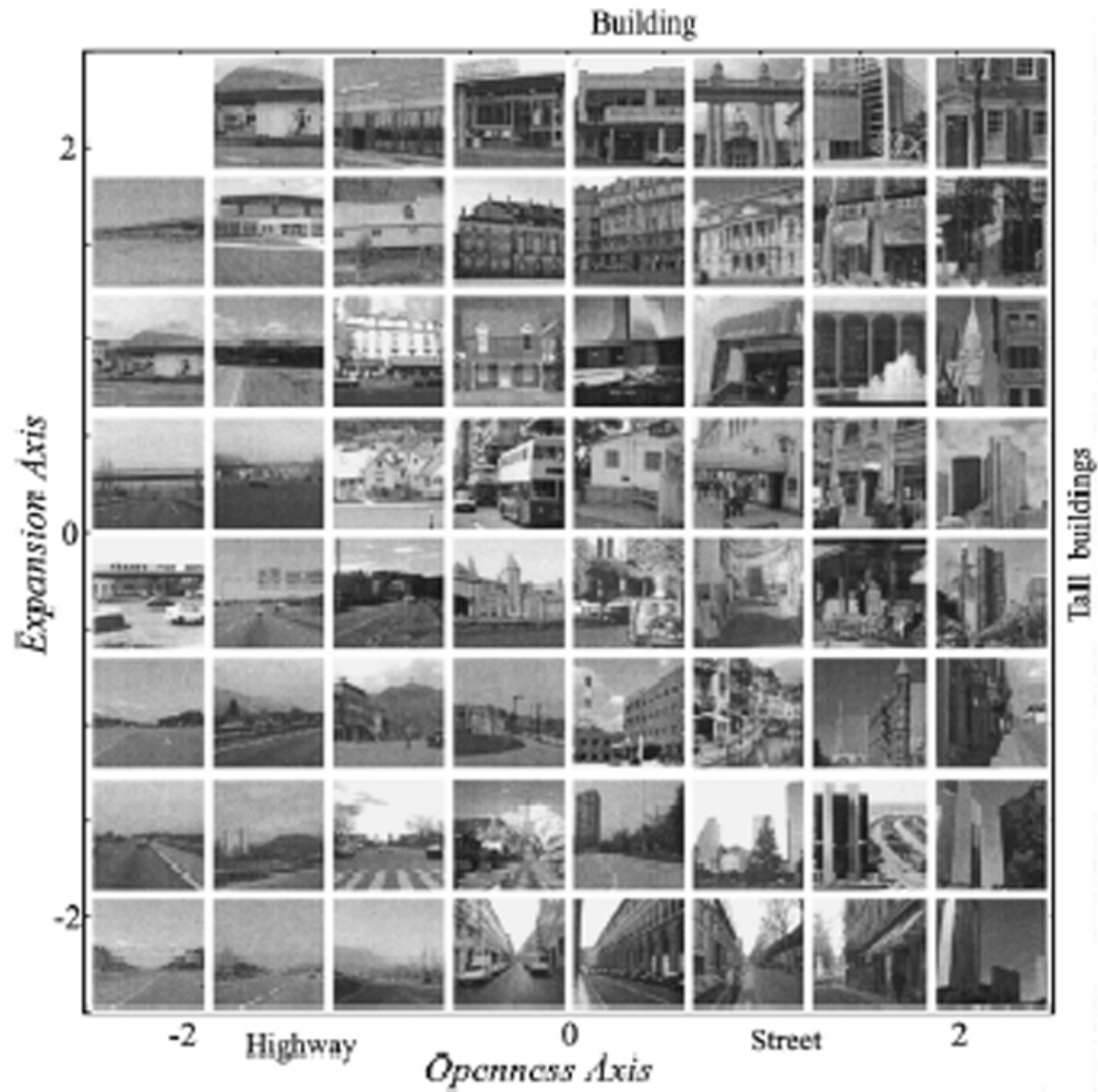


Fig. 16. Organization of man-made environments according to the degree of openness and expansion (WDST).